

Stochastic treatment of the dynamics of excitons and excitonic molecules in CuCl nanocrystals

Michio Ikezawa and Yasuaki Masumoto

Institute of Physics and Center for TARA (Tsukuba Advanced Research Alliance), University of Tsukuba, Tsukuba, Ibaraki 305, Japan

(Received 21 August 1995; revised manuscript received 17 November 1995)

Dynamics of excitons and excitonic molecules in CuCl nanocrystals were investigated by means of both picosecond time-resolved luminescence and femtosecond transient absorption. Stochastic as well as rate-equation treatments are made to explain the temporal changes of both luminescence and absorption. In the stochastic treatment, a Monte Carlo simulation is made for 10^5 nanocrystals with the initial condition that the exciton number distribution follows the Poisson distribution. The stochastic treatment satisfactorily explains all the experimental results, while the rate-equation treatment does not. Success of the stochastic treatment shows the unique property of the dynamics of excitons and excitonic molecules in quantum dots arising from discreteness of the exciton number. [S0163-1829(96)04120-3]

I. INTRODUCTION

Semiconductor nanometer-size microcrystallites (nanocrystals) have attracted considerable attention, since the quantum size effect was observed in them.¹⁻⁴ They are considered to be hopeful as nonlinear optical materials and laser materials. In semiconductor nanocrystals, three-dimensional confinement of carriers is fulfilled and is expected to give the system more gain for lasing. In fact, the high optical gain and the lasing due to excitonic molecules have been observed in CuCl nanocrystals embedded in NaCl crystals.⁵ Dynamics of excitons and excitonic molecules confined in quantum dots are expected to be different from those in bulk materials. The difference should be clarified by the careful time-resolved investigation. This leads to understanding characteristic dynamics of excitons and excitonic molecules in quantum dots.

The CuCl quantum dot is an ideal system for the investigation of the dynamics of excitons and excitonic molecules confined in quantum dots, because excitons and excitonic molecules are most stable in this material and because the confinement modifies little the envelope wave function of excitons. Over the past few years, ultrafast optical measurements such as time-resolved luminescence^{6,7} and pump-and-probe measurement⁸⁻¹⁰ have been made on CuCl nanocrystals by using picosecond or subpicosecond laser pulses. However, we are confronted by difficulties in understanding the dynamics of excitons and excitonic molecules in nanocrystals. The difficulty is in the explanation of the experimental result of time-resolved luminescence of CuCl nanocrystals embedded in a NaCl crystal.⁶ The authors had attempted to fit the rate-equation calculation to the luminescence temporal changes of both the Z_3 exciton and the excitonic molecule. To explain the experimental result, they had to assume that excitonic molecules are created by pump laser pulses instantaneously as well as by excitons. This is a questionable assumption, since excitonic molecules are thought to be formed from two excitons under the excitation of the exciton band. Another difficulty is in the interpretation of the result of the pump-and-probe measurement.⁸ The authors have measured the transient absorption change and time-resolved luminescence of CuCl nanocrystals embedded in a NaCl crystal under the band-to-band excitation at 77 K. A strange

point to be noted is that the quick rise of excitonic molecule luminescence is not associated with the quick decay of exciton luminescence. The quick rise of excitonic molecule population is explained by the fast formation rate of excitonic molecules. However, the fast formation rate simultaneously gives the quick decay of the exciton population. This contradicts the experimental result.

We have faced these difficulties on the basis of the rate-equation analysis of excitons and excitonic molecules. In the rate-equation analysis, number densities of excitons and excitonic molecules, which are defined by the ensemble average number of excitons and excitonic molecules in nanocrystals, are treated as continuous real numbers. However, it must be noticed that the number of excitons and excitonic molecules in nanocrystals should be not continuous real numbers, but discrete integers. Under the sufficiently low-density excitation, the exciton number in most nanocrystals is 0 or 1. If more than 2 excitons exist in a nanocrystal, excitonic molecules can be formed. However, if only 1 exciton exists in a nanocrystal, excitonic molecule formation will never occur. On the other hand, even if the number density of the exciton is 1, the excitonic molecule formation term works in the rate-equation analysis. Hence, this discreteness should modify the dynamics of the exciton-excitonic molecule system in quantum dots from those derived by the rate-equation analysis. However, the influence has not been clarified yet.

In this study, we measured time-resolved luminescence of excitons and excitonic molecules in CuCl nanocrystals. Simultaneously, we measured the transient absorption change by means of the pump-and-probe method under exactly the same excitation condition. Both of these data are consistently explained by a stochastic model. This model describes the dynamics of excitons and excitonic molecules in nanocrystals by means of Monte Carlo simulation with the initial condition that the exciton number distribution follows the Poisson distribution.

II. EXPERIMENTAL PROCEDURES

The excitation laser source was a self-mode-locked titanium sapphire laser and a titanium sapphire regenerative am-

plifier. The output energy was $100 \mu\text{J}$, the pulse duration approximately 300 fs, and the repetition rate 1 kHz. The amplified output of the laser pulses was converted to its second harmonic, and the second-harmonic near-ultraviolet pulses were used as excitation pulses. Peak energy of the excitation pulse was 3.27 eV, corresponding to the slightly high-energy side of the Z_3 exciton structure of the sample. The exciting beam was focused on the sample surface with a spot diameter of $200 \mu\text{m}$, and the maximum power density was estimated to be $1.6 \text{ mJ}/\text{cm}^2$. For the time-resolved luminescence studies, a double monochromator with subtractive dispersion and a synchroscan streak camera were used. Time resolution of the measurement was about 30 ps. For the pump-and-probe measurement, the same excitation pulses were used for the pump pulses under the same excitation condition. Here the same excitation condition means that exactly the same optical alignment was used for both the time-resolved experiment and the pump-and-probe experiment.¹¹ A part of the amplified output of the laser pulses was focused in a sapphire crystal to generate the white continuum; the filtered output of the white continuum was used as a probe beam. This probe beam covered the spectral region down to 360 nm. The time-resolved transmission spectra were recorded by a spectrometer and a liquid-nitrogen-cooled CCD (charge-coupled device) multichannel detector. Chirping due to the group velocity dispersion in optical elements is corrected in our analysis.

A single crystal of NaCl heavily doped with CuCl was prepared by means of the transverse Bridgman method. CuCl nanocrystals were grown by means of the heat treatment performed upon the heavily doped single crystal.¹² The crystal was cleaved into small pieces of $5 \text{ mm} \times 5 \text{ mm} \times 110 \mu\text{m}$. The mean radius of nanocrystals was estimated by small-angle x-ray scattering measurement and was found to be 4.2 nm. The sample was immersed directly into liquid nitrogen in an optical cryostat.

III. NUMERICAL ANALYSIS, EXPERIMENTAL RESULTS, AND DISCUSSIONS

In bulk CuCl crystals, population dynamics of excitons and excitonic molecules have been well described by the following rate equations:^{13,14}

$$\frac{dN_{\text{ex}}}{dt} = -\frac{1}{\tau_{\text{ex}}} N_{\text{ex}} - 2\alpha N_{\text{ex}}^2 + \frac{1}{\tau_m} N_m,$$

$$\frac{dN_m}{dt} = -\frac{1}{\tau_m} N_m + \alpha N_{\text{ex}}^2.$$

Here N_{ex} and N_m are number density of excitons and excitonic molecules normalized by the number density of excitons at time zero, respectively, and the parameter α is the formation rate of excitonic molecules. τ_{ex} and τ_m are the radiative lifetime of excitons and excitonic molecules, respectively. The second term of the right-hand side of these equations represents an excitonic molecule formation process as a result of the interaction between two excitons. Numerical solutions of these rate equations for α ranging from 1/ns to 1000/ns under the initial conditions, $N_{\text{ex}}(0)=1$, and $N_m(0)=0$, are shown in Fig. 1.

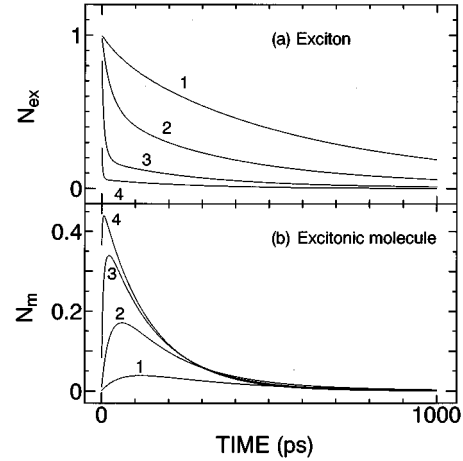


FIG. 1. Numerical solutions of rate equations shown in the text under the initial conditions, $N_{\text{ex}}(t=0)=1$ and $N_m(t=0)=0$. Curves 1, 2, 3, and 4 correspond to $\alpha=1, 10, 100$, and $1000/\text{ns}$, respectively. The upper figure shows the temporal change of the exciton density, while the lower figure that of the excitonic molecule density. The other parameters used are $\tau_{\text{ex}}=800 \text{ ps}$ and $\tau_m=70 \text{ ps}$.

Figure 2 shows the temporal changes of the luminescence of the Z_3 exciton and the excitonic molecule and time-integrated luminescence spectrum under the excitation density of $810 \mu\text{J}/\text{cm}^2$. The Z_3 exciton denoted in Fig. 2 is the lowest exciton in two series of excitons, Z_3 and $Z_{1,2}$, in CuCl made up of a common Γ_6 electron state and two different

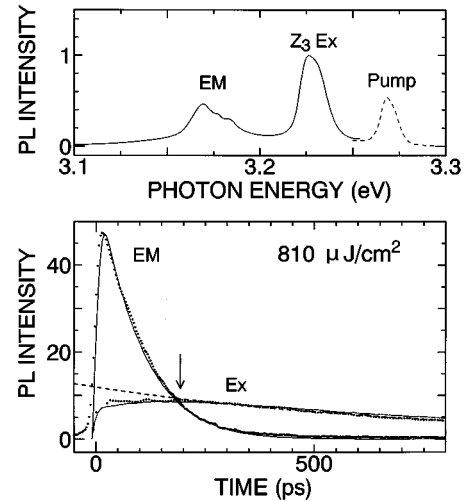


FIG. 2. Upper figure: time-integrated luminescence spectrum of CuCl nanocrystals embedded in a NaCl crystal under the excitation density of $810 \mu\text{J}/\text{cm}^2$ (solid line). The dashed line shows the excitation laser spectrum. Lower figure: temporal change of the luminescence intensity of exciton and excitonic molecule indicated by dotted lines. Exciton luminescence shows a delayed peak indicated by an arrow, while excitonic molecule luminescence has a short rise time within the experimental time resolution. A dashed line indicates the exponential decay with decay time constant of 800 ps. A solid line shows the results of the Monte Carlo simulation described in the text. The fitting is good for temporal changes of both excitons and excitonic molecules.

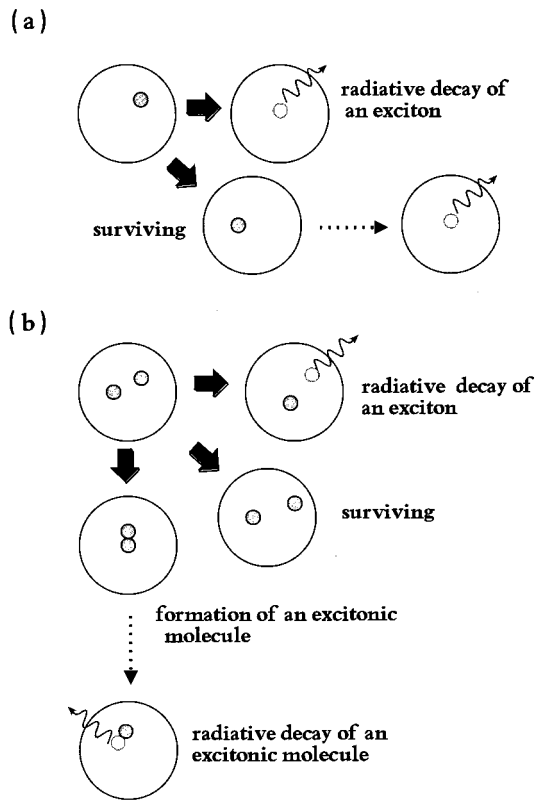


FIG. 3. Schematic explanation of the Monte Carlo simulation. (a) The case that one exciton exists in a nanocrystal. In the next step, the exciton will decay radiatively with probability $1/\tau_{\text{ex}}$ or continue surviving. (b) The case that more than two excitons exist. In the next step, the exciton will decay radiatively, continue surviving, or form an excitonic molecule with probability $1/\tau_f$. Thereafter, the excitonic molecule will decay radiatively leaving an exciton behind with probability $1/\tau_m$. If another exciton exists in the nanocrystal, an excitonic molecule may be formed again.

hole states.¹⁵ A Γ_7 hole and a Γ_6 electron make the Z_3 exciton, while a Γ_8 hole and a Γ_6 electron make the $Z_{1,2}$ exciton. The time-resolved exciton luminescence intensity shows a delayed peak at about 200 ps and thereafter decays exponentially with a decay time of 800 ps. On the other hand, excitonic molecule luminescence rises quickly within the time resolution of 30 ps and decays with a decay time of 70 ps. The important point to be noted is that the delayed peak of exciton luminescence and the rapid rise of excitonic molecule luminescence are observed simultaneously.

As we have mentioned before, we must assume that excitonic molecules are instantaneously created by pump laser pulses to explain the quick rise of excitonic molecule luminescence by means of the rate-equation analysis. Otherwise, a parameter α should be very large in an order of 100/ns for the explanation of the observed rapid rise of excitonic molecule luminescence. Then, however, we cannot explain the delayed peak in the temporal change of exciton luminescence, as is shown in Fig. 1. Further, the rate-equation analysis cannot derive the delayed peak for arbitrary value of α .

We have analyzed the experimental result on the stochastic model by means of the Monte Carlo simulation¹⁶ of the temporal change of excitons and excitonic molecules. The

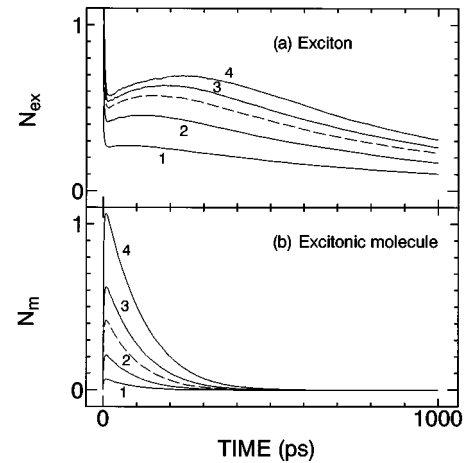


FIG. 4. Solid lines show the results of the Monte Carlo simulation. The temporal change of the exciton number density is shown in (a), while that of excitonic-molecule number density is shown in (b). Curves 1, 2, 3, and 4 correspond to $\lambda=0.5, 1.0, 2.0,$ and $3.0,$ respectively. Delayed peaks are observed in (a). Dashed lines correspond to $\lambda=1.5$ and they are used to fit the temporal luminescence intensities in Fig. 2.

details of the simulation are as follows: At $t=0$, the numbers of excitons in nanocrystals follow the Poisson distribution. The size distribution of the nanocrystals is not considered. We assume that excitons cannot travel from one nanocrystal to other nanocrystals. If the number of excitons in a nanocrystal is 1, there are only two possibilities in the next time step. One is that the exciton will decay radiatively with a probability of $1/\tau_{\text{ex}}$ and the other is that the exciton continues surviving with a probability of $1 - 1/\tau_{\text{ex}}$. On the other hand, if more than two excitons exist in a nanocrystal, excitonic molecule formation occurs with a probability of $1/\tau_f$ in addition to the above-mentioned processes, as illustrated in Fig. 3. τ_f is the formation time of an excitonic molecule. We assumed the formation probability is proportional to the ratio of the effective formation volume to the total volume of a nanocrystal, where the effective formation volume for each exciton is defined by the volume of the sphere whose radius is the average distance between two excitons forming the excitonic molecule. For example, when an exciton exists in a nanocrystal and another exciton is added, the probability that the second exciton will be in the effective formation volume for the first exciton is v/V . Here V and v are given by $(4/3)\pi R^3$ and $(4/3)\pi r^3$, respectively, where R is radius of nanocrystals and $r (=1.5 \text{ nm})$ is the average distance between two excitons forming excitonic molecules.¹⁷ When two excitons exist in a nanocrystal and they do not form an excitonic molecule, the probability that a third exciton will be in the effective formation volume is $2v/V$. In this way, an excitonic molecule is formed with a larger probability from three excitons than from two excitons. Changing the excitation density corresponds to varying the mean of the Poisson distribution λ .

Now, let us compare the rate-equation analysis and the stochastic model. The results of the Monte Carlo simulation are shown in Fig. 4. Simulations are done for 10^5 nanocrystals.

tals. Solid lines in (a) and (b) are the sum of the numbers of excitons and excitonic molecules in 10^5 nanocrystals divided by the number of nanocrystals, 10^5 , respectively. Number densities are defined by them. The formation time of the excitonic molecule τ_f is 4 ps, and other parameters τ_{ex} and τ_m have the same values that are used in the rate-equation calculation. The most important difference between the result of the stochastic model and that of the rate-equation analysis is as follows: The temporal change of the number density of excitons clearly shows a delayed peak at 200 ps on the stochastic model, while it cannot be observed in the rate-equation analysis, as we have seen. The reason for this result is not so hard to see. In the stochastic model, excitonic molecules can hardly be formed after the formation time τ_f , because the exciton number is 1 or 0 in most nanocrystals. This means the exciton number density does not decrease by the excitonic molecule formation process after τ_f . It increases, however, by the radiative decay of excitonic molecules, if the number of decayed excitonic molecules is larger than the number of radiatively annihilated excitons. As a result, the delayed peak arises. On the other hand, in rate-equation analysis excitonic molecules can be formed at the nonzero rate as long as excitons exist.

Simulated number densities of radiatively annihilated excitons and excitonic molecules are plotted by solid lines in the lower part of Fig. 2. Here, convoluted curves with the time resolution of 30 ps are shown. The mean of the Poisson distribution, λ , is 1.5. The fitting is good. The delayed peak of the exciton luminescence and the rapid rise of excitonic molecule luminescence are well reproduced simultaneously. As we mentioned above, these characteristics cannot be reproduced simultaneously by the rate-equation analysis. It follows from what has been said that the discrete number of excitons in a nanocrystal affects the dynamics of excitons and excitonic molecules in a nanocrystal.

Next, let us discuss how to explain the result of subpicosecond pump-and-probe measurement by using the simulation. As we will see below, the rate-equation treatment is not suitable for the explanation of the transient absorption change. The rate-equation treatment requires that α should be very large to account for the fast rise of the optical gain observed in the transient absorption measurement, while large α simultaneously decreases the ratio of the time-integrated exciton density to that of the excitonic molecule. The small ratio contradicts the ratio used for the explanation of the observed temporal change of the blueshift of the Z_3 -exciton absorption. It also contradicts the ratio derived from the time-resolved luminescence measurement.

At the upper part of Fig. 5, a solid line and a dotted line indicate the absorption spectrum at 10 ps obtained without the pump beam and with the pump beam, respectively. The excitation density of $810 \mu\text{J}/\text{cm}^2$ is the same as is used in the time-resolved luminescence experiment. The blueshift and the broadening are observed for the Z_3 - and $Z_{1,2}$ -exciton bands. The absorption change of the $Z_{1,2}$ exciton is observed even under the Z_3 -exciton resonant excitation, because the $Z_{1,2}$ exciton and the Z_3 exciton consist of the common Γ_6 electron, as mentioned before. The time-resolved differential absorption is shown at the lower part of Fig. 5. In addition to the absorption change for the Z_3 and $Z_{1,2}$ excitons, optical gain and loss are observed at the energy of excitonic mol-

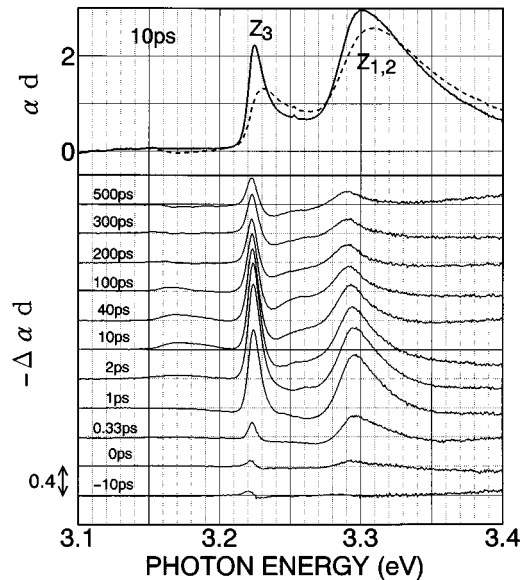


FIG. 5. The time-resolved absorption spectrum and the differential absorption spectra of CuCl nanocrystals measured by means of the pump-and-probe experiment. Upper figure: the solid line shows the absorption spectrum without the pump beam and the dashed line shows the absorption spectrum at 10 ps after the excitation. Lower figure: Differential absorption spectra at different time delays. Bleaching and optical gain are found at the energy positions of the Z_3 -exciton band and the excitonic molecule luminescence, respectively.

ecule luminescence. It was reported that a moment analysis method was useful in separating contributions of the shift and of the broadening.⁸ We also applied moment analysis to the spectra around the Z_3 and $Z_{1,2}$ excitons. It is found that saturation, that is the decrease of the zeroth moment, and

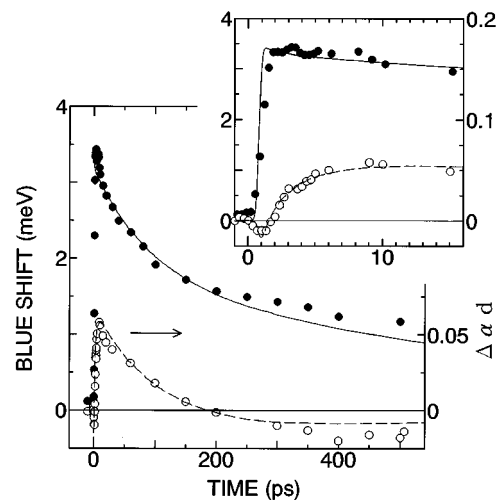


FIG. 6. Temporal changes of the blue energy shift of the Z_3 -exciton band (\bullet) and the optical gain (\circ). The inset shows the temporal changes on the expanded time scale. The solid and dashed lines show $N_{ex} + 2N_m$ and $N_m - kN_{ex}$ obtained from the result of the simulation with $\lambda = 1.5$, respectively.

broadening, that is the increase of the second moment, are observed only within 100 ps, and their decay time constant is shorter than both exciton lifetime and excitonic molecule lifetime measured by the time-resolved luminescence. They are thought to be due to the thermalization of hot excitons. After 100 ps, the absorption change of the Z_3 exciton is dominated by the blueshift, that is the increase of the first moment. The exciton blueshift is explained by the phase space filling and the exchange effect of excitons and is proportional to the exciton density.^{18,19} Thus, the population of the exciton is most directly reflected in the blueshift. Therefore we deal mainly with the peak shift of the Z_3 exciton.

The energy shift of the Z_3 -exciton band (solid circles) and the optical gain (open circles) are plotted in Fig. 6 as a function of the delay time between the pump and the probe. The blueshift of the Z_3 exciton shows the two-component decay. The decay time of the slow component agrees with the exciton lifetime measured in the luminescence experiment. On the other hand, the fast decay component agrees with the excitonic molecule lifetime. Therefore, the slow decay component of the blueshift of the Z_3 exciton is caused by excitons existing in nanocrystals, while the fast decay component is due to excitonic molecules existing in nanocrystals. The optical gain decreases with the excitonic molecule lifetime and changes to loss at 200 ps after the excitation. The optical gain comes from the induced emission due to the transition from excitonic molecule to exciton and loss comes from the induced absorption due to the inverse transition.

The inset shows the temporal change near the time origin. The maximum of the gain is attained at about 10 ps, after the blueshift of the Z_3 -exciton band reaches its maximum. This means that excitonic molecules are formed surely from excitons with a certain formation time.

We explain these experimental results on the stochastic model. The exciton blueshift comes from the phase-space filling and the exchange of an exciton. Since an excitonic molecule consists of two excitons, it is likely that an excitonic molecule contributes to the shift of the exciton band as two excitons do. In fact, the calculated curve of $N_{\text{ex}}+2N_m$ based on the simulation result with $\lambda=1.5$ agrees with the experimental result, as shown in Fig. 6. In the simulation shown in Fig. 2, the exciton population decreases rapidly due to the formation of the excitonic molecule. As far as the blueshift of the Z_3 exciton is concerned, however, the decrease is compensated by the created excitonic molecules because of the equality of an excitonic molecule and two excitons in our assumption. As a consequence, the blueshift of the Z_3 exciton decreases with the decay time constant of the lifetime of the excitonic molecule, which is the net decay time constant of $N_{\text{ex}}+2N_m$.

On the other hand, it is considered that the gain and the loss are related to the difference between numbers of excitons and excitonic molecules. We have calculated $N_m - kN_{\text{ex}}$ by using simulated values of N_{ex} and N_m , and plotted in Fig. 6 by a broken line. Temporal change of gain and loss are well reproduced, if the value of k is set to 0.12. The Z_3 -exciton states consist of a longitudinal mode and two transverse modes. The optical gain is considered to come from the population inversion between the excitonic molecule state and mainly the longitudinal exciton state. The population of the longitudinal exciton is estimated to be 0.22

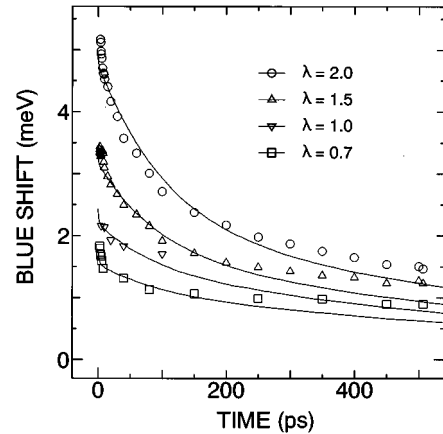


FIG. 7. Temporal change of the blueshift of the Z_3 -exciton band for four excitation densities, 1.6 mJ/cm^2 (\circ), $810 \text{ } \mu\text{J/cm}^2$ (Δ), $320 \text{ } \mu\text{J/cm}^2$ (∇), and $160 \text{ } \mu\text{J/cm}^2$ (\square). Solid lines indicate $N_{\text{ex}}+2N_m$ obtained from the results of the simulation with $\lambda=2.0$, 1.5 , 1.0 , and 0.7 , respectively.

of the transverse exciton population at 77 K considering their energy difference of 5.5 meV and multiplicity of 2 for transverse modes. The fitted value is smaller than the estimation. We cannot explain this disagreement.

In the rate-equation treatment, the parameter α should be very large to derive the fast rise of the optical gain seen in Fig. 6. However, very large α simultaneously equates the decay time of $N_{\text{ex}}+2N_m$ to the lifetime of the excitonic molecule. As a result, $N_{\text{ex}}+2N_m$ decays nearly exponentially at the lifetime of the excitonic molecule. This contradicts the observed two-component decay seen in Fig. 6.

In Fig. 7, the temporal change of the blueshift of the Z_3 exciton is plotted for four excitation densities. Increase of the fast decay component is observed with increasing the excitation density. Solid lines indicate the simulated values of $N_{\text{ex}}+2N_m$ for various λ . We obtained good fits with the experimental result for all the excitation densities by changing only λ . The ratio of excitation density is 5.0:2.5:1.0:0.5, while corresponding λ is 2.0, 1.5, 1.0, and 0.7, respectively. The number density of excitons increases with the increase of the excitation density, but the increase shows the saturation behavior. The saturation behavior is also observed in the luminescence intensity.⁵ The reason why the number density of excitons does not increase strictly in proportion to the excitation density is not clear.

Another fast decay component is found at the lowest excitation density. Its decay time is on the order of a few picoseconds, and shorter than the excitonic molecule lifetime. We can ascribe the origin of the fast component to exciton trapping at the surface state of the nanocrystal. A certain number of traps independent of excitation density was added to the simulation process. Since this component comes into prominence with decreasing excitation density, the number of traps is reasonably determined to be 10% of the total number of nanocrystals. Including the traps to the simulation has little effect on the simulated result for the higher excitation density.

IV. CONCLUSION

Time-resolved luminescence and transient absorption change were studied in CuCl nanocrystals embedded in a NaCl crystal. The observed delayed peak in the temporal change of the exciton luminescence and the rapid rise of the excitonic molecule luminescence, which could not be described by the rate-equation model, are well described by the stochastic model. The transient absorption change of the Z_3 -exciton band and the optical gain due to excitonic molecules are also explained. These results clearly indicate that the discreteness of exciton number is important to the dynamics of excitons and excitonic molecules in nanocrystals.

ACKNOWLEDGMENTS

The authors wish to thank Dr. T. Mishina and S. Katayanagi for their cooperation in the experiment. Small-angle x-ray-scattering experiments were done at the Photon Factory (PF) of the National Laboratory for High Energy Physics by the approval of the PF Advisory Committee (Proposals 92-117). They also wish to thank Professor Y. Amemiya in PF for his guidance to the small-angle x-ray scattering experiments. This work was supported in part by TARA (Tsukuba Advanced Research Alliance) project in University of Tsukuba.

-
- ¹A. I. Ekimov, A. L. Efros, and A. A. Onushchenko, *Solid State Commun.* **56**, 921 (1985).
- ²L. E. Brus, *J. Chem. Phys.* **80**, 4403 (1984).
- ³A. D. Yoffe, *Adv. Phys.* **42**, 173 (1993).
- ⁴L. Bányai and S. W. Koch, *Semiconductor Quantum Dots* (World Scientific, Singapore, 1993).
- ⁵Y. Masumoto, T. Kawamura, and K. Era, *Appl. Phys. Lett.* **62**, 225 (1993).
- ⁶Y. Masumoto, S. Katayanagi, and T. Mishina, *Phys. Rev. B* **49**, 10 782 (1994).
- ⁷A. Nakamura, H. Yamada, and T. Tokizaki, *Phys. Rev. B* **40**, 8585 (1989).
- ⁸K. Edamatsu, S. Iwai, T. Itoh, S. Yano, and T. Goto, *Phys. Rev. B* **51**, 11 205 (1995); see also T. Itoh *et al.*, *Jpn. J. Appl. Phys.* **34**, 1 (1995) and S. Yano *et al.*, *ibid.* **34**, 140 (1994). There is a questionable point between Fig. 1 and Fig. 4 of the first reference. When luminescence shows exponential decay, the total luminescence intensity is given by $\tau I(0)$, where τ is the decay time constant and $I(0)$ is the luminescence intensity at $t=0$. The ratio of the time-integrated luminescence of the Z_3 exciton to that of the excitonic molecule should be about 190:13, because τ_{ex} , τ_m , $I_{\text{ex}}(0)$, and $I_m(0)$ are 380 ps, 65 ps, 500, and 200, respectively, in Fig. 4. In the luminescence spectrum of Fig. 1, however, the ratio of the intensity is about 3.4:1. This discrepancy is too large.
- ⁹P. Faller, V. Netiksis, J. B. Grun, and B. Hönerlage, *J. Appl. Phys.* **74**, 2748 (1993).
- ¹⁰B. Kippelen, R. Levy, P. Gilliot, and L. Belleguie, *Appl. Phys. Lett.* **59**, 3378 (1991).
- ¹¹This special care was found to be important for the detailed discussion of the population dynamics of excitons and excitonic molecules. In our previous study of Ref. 6, we measured the time-resolved luminescence alone and did not measure the time-resolved absorption. In this case, the time resolution is not short enough to see directly the formation process of excitonic molecules.
- ¹²T. Itoh, Y. Iwabuchi, and M. Kataoka, *Phys. Status Solidi B* **145**, 567 (1988); T. Itoh, Y. Iwabuchi, and T. Kirihara, *ibid.* **146**, 531 (1988).
- ¹³M. Ojima, T. Kushida, Y. Tanaka, and S. Shionoya, *J. Phys. Soc. Jpn.* **44**, 1294 (1978).
- ¹⁴T. Ikehara and T. Itoh, *Solid State Commun.* **79**, 755 (1991).
- ¹⁵M. Cardona, *Phys. Rev.* **129**, 69 (1963).
- ¹⁶*Monte Carlo Simulation in Statistical Physics*, edited by K. Binder and D. W. Heermann (Springer-Verlag, Berlin, 1988).
- ¹⁷Y. Kayanuma and K. Kuroda, *Appl. Phys. A* **53**, 475 (1991).
- ¹⁸E. Hanamura, *J. Phys. Soc. Jpn.* **29**, 50 (1970).
- ¹⁹M. Ueta, K. Kobayashi, Y. Toyozawa, and E. Hanamura, *Excitonic Processes in Solids* (Springer-Verlag, Berlin, 1986).